Available online at www.sciencedirect.com

ScienceDirect

Solar Energy 102 (2014) 276–281

SOLAR ENERGY

www.elsevier.com/locate/solener

Structural, energetic and elastic properties of $Cu_2ZnSn(S_xSe_{1-x})_4$ ($x = 1, 0.75, 0.5, 0.25, 0$) alloys from first-principles computations

P.P. Gunaicha [a], S. Gangam [a], J.L. Roehl [b], S.V. Khare [b,*]

[a] Department of Electrical Engineering and Computer Science, The University of Toledo, 2801 West Bancroft Street, Toledo, OH 43606, USA
[b] Department of Physics and Astronomy, The University of Toledo, 2801 West Bancroft Street, Toledo, OH 43606, USA

Received 28 June 2013; received in revised form 11 January 2014; accepted 13 January 2014

Communicated by: Associate Editor Takhir M. Razykov

Abstract

We have computed the structural, energetic and elastic properties of the $Cu_2ZnSn(S_xSe_{1-x})_4$ ($x = 1, 0.75, 0.5, 0.25, 0$) alloys using *ab initio* density functional theory. For alloys containing both S and Se, a careful choice of permutations of positions for S and Se has to be made for accurately finding the minimum energy structure. The computed lattice constants increase as the fraction of S atoms in the unit cell decreases. However, the internal parameters did not show much variation with alloy composition. The computed elastic constants show that all alloys are mechanically stable. All the elastic constants and moduli, except C_{16}, increase in magnitude while Poisson's ratio stays the same as the S content of the alloys increases. The computed magnitudes of elastic constant C_{16} were found to be two orders of magnitude lower compared to the other elastic constants.

Keywords: CZTS; CZTSe; Density functional theory; Elastic constants

1. Introduction

The pursuit for low cost solar cell manufacturing has led to a great increase in activity in the area of thin film photovoltaics in the last decade. Several different technologies, all exhibiting high efficiency based on different materials and surface properties, have been investigated recently, such as thin film absorber materials amorphous silicon (Singh et al., 2012; Voswinckel et al., 2013; Khare et al., 1995, 2004), CdTe (Badawi et al., 2013; Ochoa-Landin et al., 2012) and $Cu(In_{1-x}Ga_x)Se_2$ (CIGS) (Gorji et al., 2012; Thongkham et al., 2013). The heavy use of toxic Cd in these technologies along with the limited and costly supply of In, Ga and Te (Andersson, 2000; USGS, 2011) has motivated the search for new, environmentally friendly, earth abundant, cost-effective replacements materials. Recent demonstration of around 10% efficient, solar cells with Cu_2ZnSnS_4 (CZTS) and $Cu_2ZnSnSe_4$ (CZTSe) as absorber layers has revived interest in these compounds (Todorov et al., 2010; Mitzi et al., 2011). The advantages of these compounds, such as their abundant supply, low cost and nontoxicity, make them important for investigation of their electronic and mechanical properties (Persson, 2010).

CZTS and CZTSe have been investigated both experimentally and theoretically. Todorov et al. have reported a solution particle approach to fabricate CZTS PV devices with over 9.6% power conversion efficiency (Todorov et al., 2010). Persson (2010) performed theoretical analysis on electronic structure and optical response of CZTS/Se and found that the kesterite phase is more stable than the

* Corresponding author. Tel.: +1 419 530 2292; fax: +1 419 530 2723.
E-mail address: submitjournals@gmail.com (S.V. Khare).

http://dx.doi.org/10.1016/j.solener.2014.01.015
0038-092X/

stannite phase of the compound. Paier et al. (2009), also found the relative stability of the kesterite structure theoretically. Gurel et al. (2011), studied the mechanical properties for the kesterite and stannite phase for CZTS and CZTSe and found the elastic constants assuming the tetragonal TI structure for kesterite. However, the kesterite phase belongs to point group $I\bar{4}$ (Persson, 2010) which belongs to the Laue tetragonal TII structure group (Lubarda, 2001).

As important fundamental understanding of this class of materials is missing from the current literature, we report on the structural, energetic and elastic properties of the $Cu_2ZnSn(S_xSe_{1-x})_4$ ($x = 1$, 0.75, 0.5, 0.25, 0) alloys using first-principles. The minimum energy configurations of the S and Se atom permutations in the unit cell, lattice constants and internal structural parameters were investigated. The single crystal elastic constants and derived mechanical properties have been computed. These properties are of significance when one tries to synthesize the material in different composition, or a multilayer structure with graded composition changes in order to make it a better absorber. Therefore they are all critical in the search for potential materials for solar cell applications. Section 2 gives details about the computational method. Sections 3 and 4 give the results of the computed lattice constants and elastic constants. Section 5 discusses the mechanical stability Section 6 concludes the paper followed by acknowledgements.

2. Computational method

We investigated the quaternary chalcogenide alloys; $Cu_2ZnSn(S_xSe_{1-x})_4$ ($x = 1$, 0.75, 0.5, 0.25, 0) using density functional theory (DFT) Hohenberg and Kohn, 1964 computations. The alloys with $x = 0$ and $x = 1$ exist in the kesterite phase which belongs to space group S_2^4 ($I\bar{4}$; Space Group 82, 2006) (USGS, 2011). We performed first-principles total energy calculations within the local density approximation (LDA) using the suit of Vienna *ab initio* simulation package (VASP) (Kresse, 1993; Kresse and Furthmuller, 1996; Kresse and Hafner, 1993a,b) codes. Core electrons were implicitly treated by ultrasoft Vanderbilt-type pseudopotentials (Vanderbilt, 1990) as supplied by Kresse and Hafner (1994). Irreducible k points were generated according to the Monkhorst–Pack scheme (Monkhorst and Pack, 1976) for each calculation. The single-particle wave functions were expanded in a plane-wave basis using a 300 eV energy cutoff. Tests using a higher plane-wave energy cutoff indicated a numerical convergence of ±1 meV and a larger k-point sampling ($4 \times 4 \times 4$) indicated that a numerical convergence better than ±2 meV was achieved. The minimum energy for each configuration was obtained by full relaxation of all the atoms until a force convergence of less than 0.005 eV/Å was achieved. Thus the error in the energy differences between different alloys was estimated to be ±10 meV. To obtain the absolute minimum in total energy, the lattice constants "a" and "c", along with the internal parameters of freedom u_i ($i = 1, 2, 3$), were varied independently. Then fits of the total energy to parabolic equations in the lattice constants were made to obtain the absolute minimum total energy for each alloy ($x = 1$, 0.75, 0.5, 0.25, 0).

The independent elastic constants (Nye, 1985) for all the alloys were computed. The procedure involved computing the total minimum energy of the crystal under strain and relaxing all the internal parameters (Patil et al., 2006, 2008). Each lattice vector, strained $\bar{a}'_k$ or unstrained $\bar{a}_k$, ($k = 1, 2, 3$) is denoted by a 3×1 column matrix. The 3×3 identity matrix is $\bar{I}$. Then the strained lattice vectors are given by $\bar{a}'_k = (\bar{I} + \bar{\bar{\varepsilon}})\bar{a}_k$. The matrix $\bar{\bar{\varepsilon}}$ is a symmetric 3×3 strain matrix defined as:

$$\bar{\bar{\varepsilon}} = \begin{bmatrix} e_1 & (e_6/2) & (e_5/2) \\ (e_6/2) & e_2 & (e_4/2) \\ (e_5/2) & (e_4/2) & e_3 \end{bmatrix} \quad (1)$$

The internal parameters of the crystal are relaxed and the total minimum energy is obtained. The crystal energy is a quadratic function of the set of strains $\{e_i\}$ (Nye, 1985). Hence, the change in the total energy of the crystal due to the applied strain is:

$$\Delta E(e_i) = \left(\frac{V}{2}\right)\sum_{i=1}^{6}\sum_{j=1}^{6} C_{ij}e_ie_j + O(e_i^3) \quad (2)$$

where V is the volume of the unstrained crystal, $O(e_i^3)$ indicates the neglected higher order terms of e_i in the polynomial expansion. The different elastic constants C_{ij} are obtained by appropriate choices of the strains that take values of ±1% and ±2%, as listed in Table 1.

Single crystal elastic constants can be further used as input to calculate mechanical properties of polycrystalline samples, typically observed in experiments. The Voigt–Reuss–Hill (VRH) approximation is a useful method (Chung and Buessem, 1967) to convert the anisotropic single crystal elastic constants into isotropic polycrystalline elastic moduli. The method is based on three independent

Table 1
Seven strain combinations in the strain tensor for calculating the seven elastic constants of the tetragonal structure shown in Fig. 1, following convention in reference (Patil et al., 2006). The seven independent elastic constants C_{11}, C_{12}, C_{13}, C_{33}, C_{44}, C_{66} and C_{16} of tetragonal cells are calculated from the above strains. Symmetry dictates $C_{ij} = C_{ji}$ and all unlisted non-equivalent $C_{ij} = 0$. The strain "δ" is varied in steps of 0.01 from $\delta = -0.02$ to 0.02. ΔE is the difference in energy between that of the strained lattice and the unstrained lattice. The equilibrium or unstrained lattice volume is V_0.

Strain	Parameters (unlisted $e_i = 0$)	ΔE
1	$e_1 = \delta$	$\frac{1}{2}C_{11}\delta^2$
2	$e_3 = \delta$	$\frac{1}{2}C_{33}\delta^2$
3	$e_4 = 2\delta$	$2C_{44}\delta^2$
4	$e_1 = 2\delta$, $e_2 = e_3 = -\delta$	$\frac{1}{2}(5C_{11} - 4C_{12} - 2C_{13} + C_{33})\delta^2$
5	$e_1 = e_2 = -\delta$, $e_3 = 2\delta$	$(C_{11} + C_{12} - 4C_{13} + 2C_{33})\delta^2$
6	$e_1 = e_2 = [1+(\delta^2/4)]^{1/2} - 1$, $e_6 = \delta$	$\frac{1}{2}C_{66}\delta^2$
7	$e_1 = e_6 = \delta$	$\frac{1}{2}(C_{11} + 2C_{16} + C_{66})\delta^2$

theoretical contributions due to Voigt (Voight, 1928; Mehl et al., 1994), Reuss (Mehl et al., 1994; Reuss, 1929) and Hill (Hill, 1952). Using the single crystal data, the isotropic bulk (B) and shear (G) moduli are computed as, $B = (B_V + B_R)/2$ and $G = (G_V + G_R)/2$. These are the arithmetic mean of the bounds on the moduli, found by Voigt and Reuss.

For a tetragonal lattice these bounds are:

$$B_R = \frac{[(C_{11}+C_{12})C_{33} - 2C_{13}^2]}{(C_{11}+C_{12}+2C_{33}-4C_{13})} \text{ and}$$

$$B_V = \frac{(2C_{11}+C_{33}+2C_{12}+4C_{13})}{9}$$

while (Mehl et al., 1994)

$$G_R = \frac{15C(C_{11}-C_{12})C_{44}C_{66}}{\{2(C_{11}-C_{12})[2(C_{11}+C_{12})+4C_{13}+C_{33}]C_{44}C_{66}+3C[2C_{44}C_{66}+(C_{11}-C_{12})(C_{44}+2C_{66})]\}}$$

and

$$G_V = \frac{(2C_{11}+C_{33}-C_{12}-2C_{13}+6C_{44}+3C_{66})}{15}$$

Here, $C = C_{33}(C_{11}+C_{12}) - 2C_{13}^2$

The Young's modulus (E) for an isotropic solid is given by Mehl et al. (1994) $E = 9BG/(3B+G)$, while the Poisson's ratio (v) is given by Mehl et al. (1994) $v = (3B-E)/(6B)$. Compressibility (K) is just the inverse of the bulk modulus (Ashcroft and Mermin, 1976) $K = 1/B$.

3. Crystal structure

The unit cell for $Cu_2ZnSn(S_xSe_{1-x})_4$, with $x = 1$, is shown in Fig. 1. This tetragonal unit cell has two lattice constants "a" and "c" with lattice vectors $\bar{a}_1 = (a, 0, 0)$, $\bar{a}_2 = (0, a, 0)$ and $\bar{a}_3 = \frac{1}{2}(a, a, 2c)$. The eight basis atom positions are given in Table 2 along with their Wyckoff positions. Alloys with $x = ¼$, ½ and ¾ contain both S and Se atoms in the unit cell. The S atoms to be replaced with Se, for the alloys, were chosen such that the resulting structure would have the minimum energy among all possible replacement combinations. By considerations of symmetry non-equivalent selections of S atoms to be replaced by Se atoms, according to the convention in Table 2, were: (i) S_1,S_2, (ii) S_2,S_4 and equivalent other combinations for $x = ½$. Not all combinations yielded the same energy for the resulting unit cell. For $x = ½$, combination (i) yielded a structure with energy higher than the combination (ii) and other equivalent combinations by at least 28 meV/cell. Similar choices needed to be made for alloys with other fractional values of x. Our computations revealed the lowest energy alloys formed with the following choices for replacement of S with Se atoms: S_1 for $x = ¾$, S_2 and S_4 for $x = ½$, S_2, S_3 and S_4 for $x = ¼$. At this stage, this small energy difference is difficult to plausibly explain away in simple geometric or phenomenological terms.

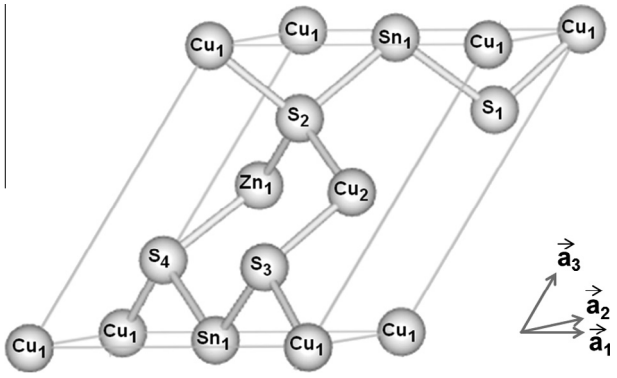

Fig. 1. The figure shows the 8-atom crystal structure of kesterite. The suffix following the element name signifies the number of the atom of the respective element present in the unit cell. Example: S_3 means the third sulfur atom present in the 8-atom unit cell. The lattice vectors are shown as $\bar{a}_1$,$\bar{a}_2$ and $\bar{a}_3$ respectively.

The computed equilibrium lattice constants and internal parameters $\{u_i,\ i = 1, 2, 3\}$ for all our alloys, are given in Table 3. The lattice parameters "a" and "c" follow a trend with the gradual substitution of S with Se. The lattice parameters "a" and "c" for the alloy $Cu_2ZnSn(S_xSe_{1-x})_4$ increase from 5.32 Å to 5.58 Å and 10.67 to 11.35 Å respectively when "x" decreases from 1 to 0. The volume of the crystal unit cell increased from 151.22 $Å^3$ to 175.74 $Å^3$ when "x" decreases from 1 to 0 in the alloy. This is the result of the larger size of the selenium atom compared to that of a sulfur atom. The three internal parameters in the unit cell do not show any such trend. They fluctuate around fractional values of $u_1 = 1/4$, $u_2 = 1/4$ and $u_3 = 9/25$. The computed equilibrium lattice constants for the alloys Cu_2ZnSnS_4 and $Cu_2ZnSnSe_4$ shown in Table 3 are in good agreement with earlier published theoretical and experimental results (Persson, 2010; Schorr et al., 2007; Hall et al., 1978; Maeda et al., 2009; Zoppi et al., 2009).

Table 2
Basis atom positions (Space Group 82, 2006) for the atoms shown in Fig. 1 along with their Wyckoff positions (Persson, 2010).

Atom type	Basis atom position	Wyckoff position
Cu_1	0	2*a*
Cu_2	$(3\bar{a}_1 + \bar{a}_2 + 2\bar{a}_3)/4$	2*c*
Zn_1	$(\bar{a}_1 + 3\bar{a}_2 + 2\bar{a}_3)/4$	2*d*
Sn_1	$(\bar{a}_1 + \bar{a}_2)/2$	2*b*
S_1	$+(u_1-u_3)\bar{a}_1 + (u_2-u_3)\bar{a}_2 + 2u_3\bar{a}_3$	8*g*
S_2	$-(u_1+u_3)\bar{a}_1 - (u_2+u_3)\bar{a}_2 + 2u_3\bar{a}_3$	8*g*
S_3	$+(u_2+u_3)\bar{a}_1 - (u_1-u_3)\bar{a}_2 - 2u_3\bar{a}_3$	8*g*
S_4	$+(u_3-u_2)\bar{a}_1 + (u_1+u_3)\bar{a}_2 - 2u_3\bar{a}_3$	8*g*

Table 3
The lattice constants of different alloys of kesterite structure of $Cu_2ZnSn(S_xSe_{1-x})_4$ obtained within the local density approximation (LDA).

$Cu_2ZnSn(S_xSe_{1-x})4$	Lattice constants (Å)		Internal parameters		
x	a	c	u_1	u_2	u_3
1	5.32	10.67	0.2597	0.2686	0.3692
	5.326[a]	10.663[a]	–	–	–
	5.428[b]	10.864[b]	–	–	–
	5.427[c]	10.871[c]	–	–	–
0.75	5.4	10.79	0.2617	0.2731	0.3688
0.5	5.46	10.94	0.262	0.2684	0.3705
0.25	5.53	11.07	0.2594	0.2665	0.3693
0	5.58	11.35	0.2608	0.2707	0.3683
	5.605[a]	11.208[a]	–	–	–
	5.692[d]	11.34[d]	–	–	–
	5.684[e]	11.353[e]	–	–	–

[a] Persson: theoretical values from reference (Persson, 2010).
[b] Schorr et al.: experimental values from reference (Schorr et al., 2007).
[c] Hall et al.: experimental values from reference (Hall et al., 1978).
[d] Maeda et al.: experimental values from reference (Maeda et al., 2009).
[e] Zoppi et al.: experimental values from reference (Zoppi et al., 2009).

4. Elastic constants

The elastic constants reduce to 21 from 36 due to crystal symmetry (Nye, 1985). Further crystal symmetry (Nye, 1985) of tetragonal (TII) crystals reduces these constants to 7 (C_{11}, C_{12}, C_{13}, C_{33}, C_{44}, C_{66}, C_{16}). The appropriate choice of strain $\{e_i\}$ leads to a parabolic relationship of Eq. (2), between ΔE and the strains. The choices of the strain for the TII crystal are shown in Table 1 (Nye, 1985) with the corresponding ΔE. Other strains (not listed) were used to over-determine and hence confirm the accuracy of the elastic constants.

The total minimum energies of the crystal under strain were obtained. For each choice of strain, shown in Table 1, we obtained a parabolic fit for Eq. (2) for ΔE vs. strain. These fits yielded linear combinations of elastic constants shown in Table 1, which were solved to obtain the individual constants C_{ij}. Elastic constants computed, by this method, for all our alloys are given in Table 4. We observe a common trend in the elastic constants for all alloys. The elastic constants follow the following order: $C_{33} \approx C_{11} > C_{13} \approx C_{12} > C_{44} \approx C_{66} > C_{16}$. We observe that C_{16} is significantly lower than the other constants. These independent elastic constants were used to derive the Voigt–Reuss–Hill approximated Bulk moduli (Chung and Buessem, 1967) (B) and Shear moduli (Chung and Buessem, 1967) (G), Compressibility (Ashcroft and Mermin, 1976) (K), Young's moduli Mehl et al., 1994 (E) and Poisson's ratio (Mehl et al., 1994) (υ) for each of the 5 compounds, $Cu_2ZnSn(S_xSe_{1-x})_4$ ($x = 1, 0.75, 0.5, 0.25, 0$) (See Table 5). The bulk and shear moduli decrease from 88.37 GPa to 73.17 GPa and 33.18–27.84 GPa respectively as "x" decreases from 1 to 0. The compressibility increases from 11.32/TPa^{-1} to 13.66/TPa^{-1} as "x" decreases from 1 to 0. There is not a significant change in the Poisson's ratio with the variation in "x". The Young's moduli decrease from 88.46 GPa to 74.12 GPa with the decrease in "x" from 1 to 0.

Table 4
The seven independent elastic constants, for each of the 5 compounds, $Cu_2ZnSn(S_xSe_{1-x})_4$, calculated using LDA.

Elastic constants of $Cu_2ZnSn(S_xSe_{1-x})_4$ in GPa					
C_{ij}	$x = 1$	$x = 0.75$	$x = 0.5$	$x = 0.25$	$x = 0$
C_{11}	114.42	109.83	104.33	99.09	95.95
C_{12}	74.51	71.54	67.84	64.36	62.80
C_{13}	75.51	71.25	67.28	65.02	61.39
C_{33}	115.41	109.54	104.45	99.52	95.54
C_{44}	47.30	44.80	43.07	40.84	38.99
C_{66}	46.14	44.37	41.39	39.73	38.39
C_{16}	0.41	0.45	0.75	0.64	0.38

Table 5
Voigt–Reuss–Hill approximated Bulk moduli (Chung and Buessem, 1967) (B) and Shear moduli (Chung and Buessem, 1967) (G), Compressibility (Ashcroft and Mermin, 1976) (K), Young's moduli Mehl et al., 1994 (E) and Poisson's ratio (Mehl et al., 1994) (υ) for each of the 5 compounds, $Cu_2ZnSn(S_xSe_{1-x})_4$. These are derived from the independent elastic constants shown in Table 4.

Material	B (GPa)	G (GPa)	K (TPa^{-1})	E (GPa)	υ
Cu_2ZnSnS_4	88.37	33.18	11.32	88.46	0.33
Cu_2ZnSnS_3Se	84.14	31.82	11.88	84.78	0.33
$Cu_2ZnSnS_2Se_2$	79.77	30.41	12.54	80.94	0.33
$Cu_2ZnSnSSe_3$	76.28	28.72	13.11	76.55	0.33
$Cu_2ZnSnSe_4$	73.17	27.84	13.66	74.12	0.33

Li et al. (2000) revealed the influence of strain on the equilibrium shape anisotropy of 2D islands growing heteroepitaxially on a substrate, or homoepitaxially with substrate surface stress anisotropy (Xu et al., 2003). The unit strain energy $E_S = \frac{1+\upsilon}{2\pi E}F^2$, where υ and E are Poisson's ratio and Young's modulus of the substrate, and F is the force density along the periphery of the island. Our computed results for υ and E can serve to estimate such surface strain energies for CZTS/Se. The values of υ stays at about 0.33,

but the values of E decrease from 88.46 GPa to 74.12 GPa as more S atoms are replaced by Se atoms in the formula, resulting in higher surface strain energy values. On one hand, the strain energy, along with the step free energy of two edges determines the shape of the island especially when it grows bigger, thus eventually influencing the domain shape of the deposited film on the substrate made of CZTS/Se. On the other hand, a bigger value of strain energy makes film deposition on the substrate more difficult and adjustment of experimental procedures should be anticipated. Apart from such effects on film growth due to influence on surface stress, many other properties in the bulk are influenced by values of the elastic constants. The nature of phonons is strongly dependent on the values and anisotropy of elastic constants. For example, elastic waves propagating through the crystal in different directions will have different velocities, thus influencing the phonon dispersion curve (Yu and Cardona, 2005). The anisotropic elastic constants we have computed directly influence such velocities and shapes of dispersion curves. Similarly, dislocation formation, their elastic fields and motion also come under the direct influence of the elastic constants (Li et al., 2004). Furthermore, formation and migration of point defects such as vacancies is also influenced by the ability of a bulk crystal to sustain stresses which may come about due to interface lattice mismatches or other processing steps in any solar cell (Botez et al., 2002). Several other thermodynamic, optical, electric and magnetic properties are also affected by the values of elastic constants (Nye, 1985; Patil et al., 2008; Liu et al., 2014).

5. Mechanical stability

For a crystal structure to be mechanically stable, the strain energy, given by Eq. (2), should be positive definite (Ferrar, 1941) for all values of strain δ. This imposes further restrictions on the elastic constants depending on the crystal structure. For the quaternary chalcogenide alloys $Cu_2ZnSn(S_xSe_{1-x})_4$ ($x = 1,\ 0.75,\ 0.5,\ 0.25,\ 0$) studied in the work the necessary conditions for the mechanical stability of the crystal are given by Monkhorst and Pack (1976) and Ferrar (1941).

$$C_{11}, C_{33}, C_{44}, C_{66} > 0, 5C_{11} - 4C_{12} - 2C_{13} + C_{33} > 0,$$

$$C_{11} + C_{12} - 4C_{13} + 2C_{33} > 0,\ C_{11} + C_{12} - 4C_{13} + 2C_{33} + 2C_{66} > 0,$$

$$C_{11} + 2C_{16} + C_{66} > 0,\ C_{11} - 2C_{16} + C_{16} > 0,\ C_{11} - C_{12} > 0,$$

$$C_{66} + \left(\frac{5}{4}C_{11}\right) - C_{12} - \left(\frac{1}{2}C_{13}\right) + 3C_{16} + \left(\frac{1}{4}C_{33}\right) + 2C_{44} > 0,\ C_{11}^2 - C_{12}^2 > 0,$$

$$\left(C_{11}^2C_{33}C_{66} - 2C_{33}C_{11}C_{16}^2 - 2C_{13}^2C_{66}C_{11} - C_{12}^2C_{33}C_{66} + 4C_{13}^2C_{16}^2 + 2C_{13}^2C_{12}C_{66} - 2C_{16}^2C_{33}C_{12}\right)C_{44}^2 > 0,$$

$$C_{11}^2C_{33} - 2C_{11}C_{13}^2 + 2C_{12}C_{13}^2 - C_{12}^2C_{13} > 0$$

and

$$(C_{11}^2C_{33} - 2C_{11}C_{13}^2 + 2C_{12}C_{13}^2 - C_{12}^2C_{13})C_{44} > 0.$$

All five alloys satisfy these conditions and are thus mechanically stable. Their fabrication in the laboratory is therefore possible. This leads to the prospect of making a multi-layer absorption layer with composition grading between S and Se fractions to capture a larger window of the solar spectrum.

6. Conclusion

We have computed the structural, energetic and elastic properties of the $Cu_2ZnSn(S_xSe_{1-x})_4$ ($x = 1,\ 0.75,\ 0.5,\ 0.25,\ 0$) alloys using first principle calculations. Careful choice of positions to replace S atoms with Se has to be made for accurately determining the minimum energy structure for mixed alloys containing both S and Se. The computed lattice constants decrease with increasing fraction of Se atoms in the unit cell. However, the internal parameters did not show much variation with alloy composition. All elastic constants except C_{16} increased in magnitude as S content increased. The magnitude of elastic constant C_{16} was found to be considerably lower compared to the other elastic constants and showed no discernible trend with change in S content in the alloy.

Acknowledgements

We thank the US National Science Foundation for funding this work with the following awards: CMMI 0928440, CMMI 1234777 and CNS 0855134. We thank the Ohio Supercomputing (OSC) center for providing computing resources. We thank Dr. Rick Irving for help with computing.

References

Andersson, B.A., 2000. Materials availability for large-scale thin-film photovoltaics. Prog. Photovoltaics 8, 61–76.

Ashcroft, N.W., Mermin, N.D., 1976. Solid State Physics. World Publishing Corporation.

Badawi, A., Al-Hosiny, N., Abdallah, S., Negm, S., Talaat, H., 2013. Tuning photocurrent response through size control of CdTe quantum dots sensitized solar cells. Sol. Energy 88, 137–143.

Botez, C.E., Li, K., Lu, E.D., Elliott, W.C., Miceli, P.F., Conrad, E.H., Stephens, P.W., 2002. Vacancy trapping and annealing in noble-metal films grown at low temperature. Appl. Phys. Lett. 81, 4718–4720.

Chung, D.H., Buessem, W.R., 1967. Voigt–Reuss–Hill approximation and elastic moduli of polycrystalline Mgo Caf_2 Beta–Zns Znse and Cdte. J. Appl. Phys. 38, 2535.

Ferrar, W.L., 1941. Algebra: A Text-Book of Determinants, Matrices, and Algebraic Forms. Oxford University Press, Oxford, UK.

Gorji, N.E., Reggiani, U., Sandrolini, L., 2012. A simple model for the photocurrent density of a graded band gap CIGS thin film solar cell. Sol. Energy 86, 920–925.

Gurel, T., Sevik, C., Cagin, T., 2011. Characterization of vibrational and mechanical properties of quaternary compounds Cu_2ZnSnS_4 and $Cu_2ZnSnSe_4$ in kesterite and stannite structures. Phys. Rev. B 84, 205201.

Hall, S.R., Szymanski, J.T., Stewart, J.M., 1978. Kesterite, $Cu_2(Zn, Fe)SnS_4$, and stannite, $Cu_2(Fe, Zn)SnS_4$, structurally similar but distinct minerals. Can. Mineral. 16, 131–137.

Hill, R., 1952. The elastic behaviour of a crystalline aggregate. Proc. Phys. Soc. A 65, 349.

Hohenberg, P., Kohn, W., 1964. Inhomogeneous electron gas. Phys. Rev. 136, B864–B871.

Khare, S.V., Einstein, T.L., Bartelt, N.C., 1995. Dynamics of step doubling – simulations for a simple-model and comparison with experiment. Surf. Sci. 339, 353–362.

Khare, S.V., Nakhmanson, S.M., Voyles, P.M., Keblinski, P., Abelson, J.R., 2004. Evidence from atomistic simulations of fluctuation electron microscopy for preferred local orientations in amorphous silicon. Appl. Phys. Lett. 85, 745–747.

Kresse, G., 1993. Ab-initio Molekular Dynamik für flüssige Metalle. Technische Universität Wien.

Kresse, G., Furthmuller, J., 1996. Efficiency of ab-initio total energy calculations for metals and semiconductors using a plane-wave basis set. Comput. Mater. Sci. 6, 15–50.

Kresse, G., Hafner, J., 1993a. Ab-initio molecular-dynamics for open-shell transition-metals. Phys. Rev. B 48, 13115–13118.

Kresse, G., Hafner, J., 1993b. Ab initio molecular dynamics for liquid metals. Phys. Rev. B 47, 558–561.

Kresse, G., Hafner, J., 1994. Norm-conserving and ultrasoft pseudopotentials for first-row and transition-elements. J. Phys.: Condens. Matter 6, 8245–8257.

Li, A., Liu, F., Lagally, M.G., 2000. Equilibrium shape of two-dimensional islands under stress. Phys. Rev. Lett. 85, 1922–1925.

Li, J., Zhu, T., Yip, S., Van Vliet, K.J., Suresh, S., 2004. Elastic criterion for dislocation nucleation. Mater. Sci. Eng. A – Struct. 365, 25–30.

Liu, Z.T.Y., Zhou, X., Khare, S.V., Gall, D., 2014. Structural, mechanical and electronic properties of 3d transition metal nitrides in cubic zincblende, rocksalt and cesium chloride structures: a first-principles investigation. J. Phys.: Condens. Matter 26, 025404.

Lubarda, V.A., 2001. Elastoplasticity Theory. CRC Press.

Maeda, T., Nakamura, S., Kou, H., Wada, T., Inoue, K., Yamaguchi, Y., 2009. Tech. Dig. PVSEC 19, CIG-O-44.

Mehl, M.J., Klein, B.M., Papaconstantopoulos, D.A., 1994. First principles calculations of elastic properties of metals. In: Westbrook, J.H., Fleischer, R.L. (Eds.), . In: Intermetallic Compounds: Principles and Practices, vol. 1. Wiley & Sons Ltd., pp. 195–210.

Mitzi, D.B., Gunawan, O., Todorov, T.K., Wang, K., Guha, S., 2011. The path towards a high-performance solution-processed kesterite solar cell. Sol. Energy Mater. Sol. Cells 95, 1421–1436.

Monkhorst, H.J., Pack, J.D., 1976. Special points for Brillouin-zone integrations. Phys. Rev. B 13, 5188–5192.

Nye, J.F., 1985. Physical Properties of Crystals: Their Representation by Tensors and Matrices. Clarendon Press.

Ochoa-Landin, R., Castillo, S.J., Ramirez-Bon, R., 2012. Growth from solution of CdTe films by conversion of chemically deposited cadmium oxide hydroxide films. Sol. Energy 86, 3326–3330.

Paier, J., Asahi, R., Nagoya, A., Kresse, G., 2009. Cu_2ZnSnS_4 as a potential photovoltaic material: a hybrid Hartree–Fock density functional theory study. Phys. Rev. B 79, 115126.

Patil, S.K.R., Khare, S.V., Tuttle, B.R., Bording, J.K., Kodambaka, S., 2006. Mechanical stability of possible structures of PtN investigated using first-principles calculations. Phys. Rev. B 73, 104118.

Patil, S.K.R., Mangale, N.S., Khare, S.V., Marsillac, S., 2008. Super hard cubic phases of period VI transition metal nitrides: first principles investigation. Thin Solid Films 517, 824–827.

Persson, C., 2010. Electronic and optical properties of Cu_2ZnSnS_4 and $Cu_2ZnSnSe_4$. J. Appl. Phys. 107, 053710.

Reuss, A., 1929. Berechnung der Fließgrenze von Mischkristallen auf Grund der Plastizitätsbedingung für Einkristalle. ZAMM – J. Appl. Math. Mech./Z. Angew. Math. Mechanik 9, 49–58.

Schorr, S., Hoebler, H.-J., Tovar, M., 2007. A neutron diffraction study of the stannite–kesterite solid solution series. Eur. J. Mineral. 19, 65–73.

Singh, S., Kumar, S., Dwivedi, N., 2012. Band gap optimization of p–i–n layers of a-Si: H by computer aided simulation for development of efficient solar cell. Sol. Energy 86, 1470–1476.

Space group 82, 2006. In: Hahn, T. (Ed.), International Tables for Crystallography Volume A: Space-group symmetry. Springer, pp. 342–343.

Thongkham, W., Pankiew, A., Yoodee, K., Chatraphorn, S., 2013. Enhancing efficiency of Cu(In, Ga)Se-2 solar cells on flexible stainless steel foils using NaF co-evaporation. Sol. Energy 92, 189–195.

Todorov, T.K., Reuter, K.B., Mitzi, D.B., 2010. High-efficiency solar cell with earth-abundant liquid-processed absorber. Adv. Mater. 22, E156–E159.

USGS, 2011. Commodity statistics and information. <http://minerals.usgs.gov/minerals/pubs/commodity/>.

Vanderbilt, D., 1990. Soft self-consistent pseudopotentials in a generalized eigenvalue formalism. Phys. Rev. B 41, 7892–7895.

Voight, W., 1928. Lehrbuch Der Kristallphysik. Johnson Reprint Corp..

Voswinckel, S., Wesselak, V., Lustermann, B., 2013. Behaviour of amorphous silicon solar modules: a parameter study. Sol. Energy 92, 206–213.

Xu, G.J., Khare, S.V., Nakayama, K.S., Aldao, C.M., Weaver, J.H., 2003. Step free energies, surface stress, and adsorbate interactions for Cl–Si(100) at 700 K. Phys. Rev. B 68, 235318.

Yu, P.Y., Cardona, M., 2005. Vibrational properties of semiconductors, and electron–phonon interactions. In: Fundamentals of Semiconductors: Physics and Materials Properties. Springer.

Zoppi, G., Forbes, I., Miles, R.W., Dale, P.J., Scragg, J.J., Peter, L.M., 2009. $Cu_2ZnSnSe_4$ in film solar cells produced by selenisation of magnetron sputtered precursors. Prog. Photovoltaics 17, 315–319.